Positron annihilation in II–VI compound semiconductors: theory

F Plazaola†, A P Seitsonen‡ and M J Puska‡

† Elektrika eta Elektronika Saila, Euskal Herriko Unibertsitatea, 644 pk, 48080 Bilbo, Spain
‡ Laboratory of Physics, Helsinki University of Technology, SF-02150 Espoo, Finland

Abstract. Positron states and annihilation rates are calculated for nine different II–VI compound semiconductors. Positron annihilation from the delocalized states in the perfect lattice as well as from the localized states at vacancies and divacancies is considered. The calculations are based on the local-density approximation (LDA) for the electron–positron correlation effects. The calculations are performed using non-self-consistent electron densities and electrostatic potentials obtained by atomic superposition and solving for the three-dimensional positron wavefunctions by a relaxation method. For the perfect lattices, also self-consistent electron densities and positron states (linear muffin-tin orbital method within atomic-spheres approximation, LMTO-ASA) are calculated. The results show that positron annihilation with the outer d electrons of the group II metal atoms plays an important role. The positron lifetimes calculated for perfect lattices are a few per cent shorter than the experimental ones, indicating an LDA overestimation of the d-electron enhancement around the positron. These bulk lifetimes can be corrected efficiently by a semiempirical model introduced in this work. In the case of positrons trapped by defects, the present theoretical description is less satisfactory, because atomic relaxations due neither to rearrangements in the electronic structure nor to the localized positron are taken into account. However, the calculated annihilation probabilities with core and valence electrons will serve as an important database for methods in which defects can be identified using the positron angular correlation or Doppler broadening measurements.

1. Introduction

During the last few years, positron annihilation techniques have proved to be valuable tools for studying atomic size defects and their interactions in semiconductors. Most of the theoretical and experimental positron work has focused on Si [1–3] and the III–V compound semiconductors [4–6]. The understanding of defect structures and the positron behaviour in these semiconductors has increased significantly. Recently, several groups have started to study II–VI compound semiconductors by positron annihilation techniques [7–16]. However, as in the case of other compound semiconductors, the interpretation of the experimental results is far from trivial. This is because, in the II–VI compound semiconductors, native point defects exist in both sublattices [17]. For example, in CdTe, vacancies on Cd or Te sites (V_{Cd}, V_{Te}), Cd or Te interstitials (Cd_i, Te_i) and antisite defects (Cd_{Te}, Te_{Cd}) can in principle be formed during crystal growth at high temperatures. During cooling down to room temperature, defects can agglomerate to form complexes with each other, with dopants or with residual impurities. Depending on the position of the Fermi level, the defects can be either neutral, or negatively or positively charged, which leads to dramatically different trapping characteristics.

Being aware of the experimental difficulties in extracting the annihilation parameters related to the bulk and to different point defects in the II–VI compound semiconductors, our aim is to support by theoretical work the interpretation of the experimental results, especially the identification of the vacancy defects belonging to the two sublattices. Therefore we calculate the lifetimes for positrons in delocalized states as well as for positrons trapped by both types of vacancies and by nearest-neighbour divacancies. It is not always easy to decompose the measured positron lifetime spectra into more than one component [8, 10] and determine the lifetime for the trapped positrons. This makes it very hard to obtain information about the vacancy-type defect involved and its identification is difficult. However, the core-electron contribution (or the high-momentum contribution) measured by angular correlation or Doppler broadening techniques can also be used in the identification of vacancy-type defects [18–20]. This method is very valuable in positron studies of thin semiconductor overlayers requiring the use of slow positron beams equipped with Doppler broadening measurement facilities. The identification is based on the fact that, in the case of the II–VI compound semiconductors, the atoms neighbouring the vacancies in the different sublattices have quite different core-electron structures. In the case of group VI atom vacancies (V_{VI}), the neighbouring atoms belong to group II, and because of their outer d electrons they have a relatively extended core. On the contrary, the group VI atoms neighbouring group II vacancies (V_{II}) have a smaller core. These differences in the core structure will be reflected in the momentum distributions of the core electrons. The divacancies may also be identified owing to the reduction of the core annihilation relative to the monovacancies. In order to study the potential of this new defect identification method, we focus our attention on the annihilation rates with the core electrons in the different vacancies, comparing them with the corresponding values for the perfect bulk lattice.

From the theoretical point of view, positron annihilation in II–VI compound semiconductors is also interesting. The highest d bands corresponding to group II atoms are usually slightly separated from the valence band and lie above the band corresponding to the outer s electrons of the group VI atoms [21–23]. Therefore, the d electrons may play an important role in determining the positron annihilation characteristics for the II–VI compound semiconductors. The comparison of the theoretical results with experiments serves as a check on the validity of the local density approximation (LDA) for the positron annihilation rate and also the validity of the proposed models for positron screening in the presence of a band gap [23].

2. Calculation methods

The present calculations for the positron states and annihilation in perfect and defective lattices of II–VI compound semiconductors have been performed using the superimposed-atom model of Puska and Nieminen [24]. For the perfect lattices we have also employed the self-consistent linear muffin-tin orbital method within the atomic-spheres approximation (LMTO-ASA) (for a recent review, see [25]). In the calculations the positron does not affect the electron structure beyond the short-range enhancement of the electron density at the positron. For the delocalized positron states, this is the correct limit of the two-component density-functional theory [26] used to describe electron–positron systems. In the case of a localized positron state at a defect, the positron density also affects the average electron density, and the electron and positron densities should be calculated simultaneously and self-consistently within the two-component density-functional theory. The approximation that we have made here is not, however, very severe, because, in the calculation of the

positron annihilation rates, neglecting the accumulation of the average electron density is compensated by a stronger short-range enhancement of the electron density [26]. A more severe approximation that we have made is that the relaxation of the atoms surrounding the vacancy defects is not taken into account. A reliable calculation of the atomic relaxations is a quite difficult task (see e.g. [27] for vacancies in GaAs). Moreover, one should take into account that a positron trapped by the defect can change the atomic relaxations [28]. In the present work we are more interested in the general trends than the detailed calculation of the positron annihilation rate for a given vacancy defect. This justifies other approximations made.

The superimposed-atom model retains the three-dimensional character of the atomic arrangement and the positron state. The electron density $n_-(r)$ and the Coulomb potential $V_C(r)$ of the host system are obtained from the free-atom densities and potentials as

$$n_-(r) = \sum_i n^{at}(|r - R_i|) \qquad V_C(r) = \sum_i V_C^{at}(|r - R_i|) \qquad (1)$$

where the summations run over the occupied atomic sites, and n^{at} and V_C^{at} are the atomic electron density and Coulomb potential, respectively. Thus, the electron density and the Coulomb potential for the solid are non-self-consistent. The three-dimensional potential $V_+(r)$ felt by the positron is then constructed as a sum of the electrostatic potential $V_C(r)$ due to the nuclei and the electrons, and a correlation potential V_{corr} describing electron–positron correlation effects, i.e.

$$V_+(r) = V_C(r) + V_{corr}(n_-(r)). \qquad (2)$$

Within LDA, V_{corr} depends on the local electron density unperturbed by the positron. For the density dependence of V_{corr} the parametrization by Boronski and Nieminen [26] has been used. It is based on the many-body results by Arponen and Pajanne [29]. The free-atom electron densities needed for the construction have been calculated relativistically by a self-consistent density-functional program employing LDA for the electron exchange and correlation [30, 31].

The calculations of the positron states with the atomic superposition method have been performed by the supercell approach employing periodic boundary conditions for the positron wavefunction. The supercell is a cube containing eight atoms in the case of a perfect lattice. In the case of a monovacancy and a divacancy it contains 215 and 214 atoms, respectively. We have noticed that for these semiconductors such large supercell sizes are necessary in order to overcome the problem of artificial defect–defect interactions caused by the periodic boundary conditions. The positron potential (equation (2)) is calculated at the nodes of a three-dimensional mesh within the cubic supercell. The Schrödinger equation is discretized, and the positron wavefunction at the mesh points of the supercell and the positron energy eigenvalue are solved iteratively by a numerical relaxation method [32].

In the LMTO-ASA calculations the electron density and Coulomb potential are determined self-consistently within spheres centred around the nuclei and the interstitial tetrahedral sites of the zincblende structure. The spheres fill the whole lattice space and they have equal radii. The electron bands corresponding to the uppermost s, p and d electrons of the group II atoms and the uppermost s and p electrons of the group VI atoms have been calculated self-consistently, whereas for the electrons deeper in the core the frozen-core approximation has been used. The potential felt by a positron is constructed according to equation (2) and the positron state is solved using the same methods as used for electron states in the LMTO-ASA.

Both in the superimposed-atom as well as in the LMTO-ASA calculations the positron annihilation rate is calculated using the LDA as

$$\lambda_{\text{LDA}} = \int dr \, |\Psi_+(r)|^2 \Gamma(n_-(r)) \tag{3}$$

where $|\Psi_+(r)|^2$ is the positron density and $\Gamma(n)$ is the annihilation rate for a positron in a homogeneous electron gas. We use for $\Gamma(n)$ the interpolation formula by Boronski and Nieminen [26], modified in order to take into account the lack of complete positron screening in semiconductors [33], i.e.

$$\Gamma(n(r)) = \pi r_0^2 cn[1 + 1.23 r_s + 0.8295 r_s^{3/2} - 1.26 r_s^2 + 0.3286 r_s^{5/2} + (1 - 1/\epsilon_\infty)(r_s^3)/6] \tag{4}$$

where r_0 is the classical electron radius, c is the velocity of light, $r_s = (3/4\pi n)^{1/3}$ and ϵ_∞ is the high-frequency dielectric constant.

In order to analyse further the positron annihilation characteristics, we have divided the total annihilation rate into different contributions (λ_i) due to the different contributions (n_i) to the total electron density. This is done following the work of Jensen [34] as

$$\lambda_i = \int dr \, |\Psi_+(r)|^2 \Gamma(n_-(r)) \frac{n_i(r)}{n_-(r)}. \tag{5}$$

Above, the density n_i corresponds to the core, valence or outer d electrons in the compound. In the present calculations the valence-electron density consists of the uppermost s and p electrons of the group II and group VI atoms. We can also calculate the contributions due to the core and the outer d electrons of the group II and group VI atoms separately.

Furthermore, following Jensen [34], the enhancement factors (γ_i) for the different electron contributions are defined as

$$\gamma_i = \lambda_i / \lambda_i^{\text{IPM}} \tag{6}$$

where λ_i^{IPM} is the corresponding annihilation rate within the independent-particle model (IPM), i.e. they are calculated as in equation (5), but $\Gamma(n_-(r))$ substituted by

$$\Gamma^{\text{IPM}}(n(r)) = \pi r_0^2 cn. \tag{7}$$

In the above definitions it is assumed that the enhancement factor does not depend on the energy of the annihilating electron, as it should according to theory and experiments [35]. Therefore, the enhancement factors calculated using equation (6) are average quantities.

We have taken into account the contribution of the outer d electrons separately, because in the case of group II atoms the annihilation rate of these electrons can be large. Thus, by means of equations (5) and (6) we are able to estimate their contribution to the total annihilation rate and, consequently, to the Gaussian (core) contribution in the momentum distribution of the annihilating pair.

3. Positrons in perfect lattices

3.1. General trends

The lattice constants and high-frequency dielectric constants used in the present calculations are listed in table 1 [21], as well as the reported experimental bulk lifetimes, i.e. the lifetimes

Table 1. Data for the II–VI compound semiconductors. The lattice constants a [20], high-frequency dielectric constants ϵ_{∞} [20] and experimental positron bulk lifetimes τ_{exp} are given. τ_{exp}^{*} is the 'average' experimental positron bulk lifetime used in comparing the theoretical and experimental results. The metal lattice constants correspond to FCC lattices built with the Wigner–Seitz volumes of the experimental lattices.

Host	a (au)	ϵ_{∞}	τ_{exp} (ps)	τ_{exp}^{*} (ps)
ZnS	10.22	5.1–5.7	230[a]	230
ZnSe	10.71	5.4–6.3	240[a]	240
ZnTe	11.53	7.28	266[b]	266
CdS	11.01	5.32		
CdSe	11.44	5.8		
CdTe	12.25	7.1–7.4	278[c],281[d],283[e],285[f],291[g]	284
HgS	11.06	7.9–9.9		
HgSe	11.50	12–21		
HgTe	12.21	15.2	274[d]	274
Zn (FCC)	7.43		148[h]	148
Cd (FCC)	8.36		175[i]	175
Hg (FCC)	8.54		182[j]	182

[a] [15], [b] [16], [c] [12], [d] [8], [e] [13], [f] [14], [g] [7], [h] [47], [i] [48], [j] [49].

for the delocalized positrons. All the results presented below have been calculated using the smallest value of the high-frequency dielectric constant presented in table 1 for the compound semiconductor in question. The use of larger dielectric constants decreases the calculated positron lifetimes values. However, the difference is relatively small. For example, in the case of HgSe using the maximum value of $\epsilon_{\infty} = 21$ instead of $\epsilon_{\infty} = 12$ decreases the bulk lifetime value by only 4 ps.

We draw general conclusions on the positron annihilation characteristics mainly on the basis of the results obtained by using the atomic superposition method. In order to get an idea of the effects of self-consistency of the electron density, we compare in table 2 the atomic superposition results for the positron bulk states with those obtained by using the LMTO-ASA method, i.e. by using self-consistent electron densities. The atomic superposition gives typically slightly longer positron lifetimes than the LMTO-ASA. This can be understood on the basis of the (valence) charge transfer from the core to the interstitial regions when the non-self-consistent electron density is substituted by the self-consistent one [33]. However, the effect is quite small, less than 2 ps for these semiconductors. Table 2 shows also the division of the annihilation rates into valence and core parts. The valence contribution λ_v' corresponds here to the uppermost s, p and d electrons of the group II atoms and to the uppermost s and p electrons of the group VI atoms. This division obeys the treatment of the electrons as the frozen core and as the valence-band electrons in the LMTO-ASA calculations. The two contributions depend weakly on the self-consistency of the electron structure. Thus the comparison in table 2 gives credence to the use of the simple atomic superposition method. This is important because the large supercells needed for the vacancy calculation can in practice be handled only with this method.

Figure 1 shows the positron bulk lifetimes obtained by the atomic superposition method as a function of the volume per atom in the zincblende structure. The figure shows that it is natural to divide the II-VI compound semiconductors into the Zn, Cd and Hg series. It is seen that within each series the positron bulk lifetime increases with the mass of the

Table 2. Positron annihilation characteristics for the perfect lattices calculated using the atomic superposition (NSC) and the LMTO-ASA (SC) methods. λ'_v is the annihilation rate with the uppermost s, p and d electrons of the group II atoms and with the uppermost s and p electrons of the group VI atoms or in the case of the LMTO-ASA calculations the annihilation rate with the electrons on the corresponding valence bands. λ'_c is the annihilation rate with the rest of the electrons (core electrons). τ is the positron lifetime.

Host	λ'_c (NSC) (ns^{-1})	λ'_v (NSC) (ns^{-1})	τ (NSC) (ps)	λ'_c (SC) (ns^{-1})	λ'_v (SC) (ns^{-1})	τ (SC) (ps)
ZnS	0.175	4.398	219	0.175	4.421	218
ZnSe	0.226	4.050	234	0.227	4.068	233
ZnTe	0.247	3.680	255	0.245	3.703	253
CdS	0.163	3.971	242	0.166	3.994	240
CdSe	0.199	3.736	254	0.203	3.750	253
CdTe	0.209	3.407	276	0.208	3.417	276
HgS	0.170	4.195	229	0.168	4.210	228
HgSe	0.204	3.989	239	0.201	3.993	238
HgTe	0.220	3.666	257	0.213	3.669	258

group VI atom. This reflects the increase of the interstitial open volume for positrons. The increasing trends for the positron lifetime are similar for the Zn, Cd and Hg series, but there is a small shift towards longer lifetimes between the Zn and Cd series and a remarkable shift towards shorter lifetimes between the Cd and Hg series.
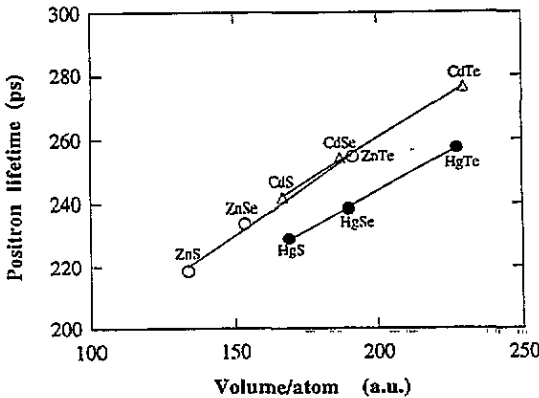

Figure 1. Positron bulk lifetimes in the II–VI compound semiconductors as a function of the volume per atom in the lattice.

The more detailed trends in the annihilation characteristics are shown in tables 3 and 4, which list the partial positron annihilation rates and the corresponding enhancement factors, respectively. The division of the valence annihilation rate between the group II and group VI atoms is somewhat arbitrary because the uppermost atomic s and p electrons spread into broad valence bands and thereby lose their identity as well defined atomic levels. Therefore the valence annihilation rates λ_v and enhancement factors γ_v include the uppermost s and p electrons of both the group II and group VI atoms. The annihilation rates with core electrons and with d electrons of the group VI atoms are relatively small and are not very important in discussing the trends between different II–VI compound semiconductors. The valence-electron contribution is the most important part in the total annihilation rate. Within each of the group II atom series the valence annihilation rate
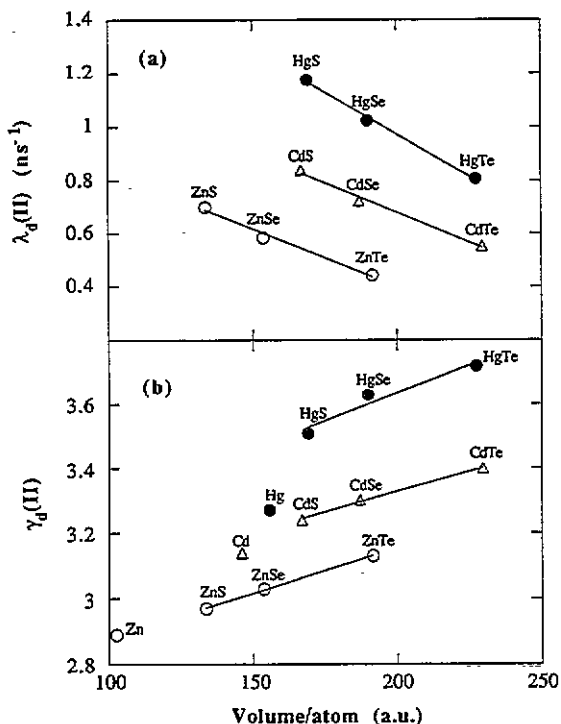
Figure 2. (*a*) Positron annihilation rate with the outer d electrons of the group II atoms in the II–VI compound semiconductors as a function of the volume per atom in the lattice. (*b*) Enhancement factors for the outer d electrons of the group II atoms in the II–VI compound semiconductors and in the FCC metals Zn, Cd and Hg as a function of the volume per atom in the lattice.

decreases when going down group VI where the lattice constant increases. There is a shift in the valence annihilation rates between the Zn and Cd series due to the increase of the lattice constants (see figure 1). In the case of the Cd and Hg series the lattice constants and consequently the valence annihilation rates for the compounds with the same group VI atom are close to each other. The valence-electron contribution can thus explain most of the changes in the total annihilation rate or in the positron lifetime within the Zn and Cd series, but it does not account for the strong decrease of the positron lifetime for the Hg series.

A prominent feature in the electron band structure of the II–VI compound semiconductors is the narrow bands corresponding to the outer d electrons of the group II atoms [21–23]. These bands lie at rather high energies in the heteropolar band gap between the uppermost group VI atom s bands and the valence bands. Therefore they are expected to have a large contribution in the annihilation rate. According to table 3 this is indeed the case, i.e. the contribution of the d electrons of the group II atoms to the total annihilation rate varies from 11% for ZnTe to 27% for HgS. The annihilation rate with the tightly bounded d electrons of the group VI atoms is much smaller. The annihilation rates with the d electrons of the group II atoms are shown in figure 2(*a*) as a function of the volume per atom. Within each series the d-electron annihilation rate decreases when the lattice constant increases. However, the annihilation rates are slightly larger for the Cd group semiconductors than for the corresponding Zn group compounds in spite of the larger lattice constants. Between the

Cd and Hg series there is a large increase in the d-electron annihilation rate. These trends reflect the increase of the spatial extent of the outer d electrons when going from the Zn series to the Cd series and further to the Hg series. A large spatial extent means a high d-electron density in the interstitial regions preferred by the positron and a large annihilation rate. The strong increase of the d-electron annihilation rate between the Cd and Hg series explains the relatively short positron lifetimes for the Hg series seen in figure 1.

Table 3. Positron annihilation characteristics for the perfect II–VI compound semiconductor and group II metal lattices. λ_c^{II} and λ_d^{II} are the annihilation rates with the core and d electrons of the group II atoms, respectively. λ_c^{VI} and λ_d^{VI} correspond to the annihilation rates with the core and d electrons of group VI atoms, respectively. λ_v is the positron annihilation rate with the valence electrons, i.e. with the uppermost s and p electrons of the group II and group VI atoms.

Host	λ_c^{II} (ns^{-1})	λ_d^{II} (ns^{-1})	λ_c^{VI} (ns^{-1})	λ_d^{VI} (ns^{-1})	λ_v (ns^{-1})
ZnS	0.144	0.700	0.031	0.000	3.698
ZnSe	0.118	0.585	0.029	0.079	3.465
ZnTe	0.086	0.443	0.031	0.130	3.237
CdS	0.141	0.841	0.022	0.000	3.130
CdSe	0.118	0.723	0.022	0.059	3.013
CdTe	0.087	0.552	0.024	0.098	2.855
HgS	0.149	1.175	0.021	0.000	3.020
HgSe	0.125	1.024	0.021	0.058	2.965
HgTe	0.095	0.808	0.024	0.101	2.858
Zn	0.632	2.769			3.849
Cd	0.534	2.827			2.997
Hg	0.515	3.457			2.552

Table 4. Enhancement factors for the perfect II–VI compound semiconductors and group II metal lattices. γ_c^{II} and γ_d^{II} correspond to the core and d electrons of the group II atoms, respectively. γ_c^{VI} and γ_d^{VI} correspond to the core and d electrons of the group VI atoms, respectively. γ_v is the enhancement factor for the valence electrons, i.e. for the uppermost s and p electrons of the group II and group VI atoms.

Host	γ_c^{II}	γ_d^{II}	γ_c^{VI}	γ_d^{VI}	γ_v
ZnS	2.02	2.97	2.03		4.24
ZnSe	2.02	3.03	1.89	2.23	4.56
ZnTe	2.03	3.13	2.05	2.53	5.21
CdS	2.20	3.24	2.07		4.69
CdSe	2.21	3.30	1.90	2.24	5.04
CdTe	2.22	3.40	2.05	2.54	5.78
HgS	2.19	3.51	2.08		4.74
HgSe	2.20	3.63	1.91	2.27	5.22
HgTe	2.21	3.72	2.06	2.57	5.89
Zn	2.05	2.89			4.03
Cd	2.22	3.14			4.48
Hg	2.19	3.27			4.33

Also the enhancement factors given in table 4 indicate the important role of the d electrons of the group II atoms The core enhancement factors vary only slightly between the different compounds. For the group II atoms they are between 2.0 and 2.2 and for the group VI atoms with more tightly bound core electrons between 1.9 and 2.1. The enhancement factors for the d electrons of the group VI atoms are somewhat above the core enhancement factors. The enhancement factors for the d electrons of the group II atoms are clearly larger, approximately in the middle between the values for the core and valence electrons. In order to study the trends of the group II d-electron enhancement factors, they are shown in figure 2(*b*) as a function of the volume per atom in the compound. The small increase of the d-electron enhancement factor within each group II series as a function of volume is a result of the decrease of average d-electron density seen by the positron. The d-electron enhancement factors increase from the Zn series to the Cd series and further to the Hg series. This reflects the increase of the spatial extent of the outer d electrons, because a more delocalized electron profile means a lower average electron density, causing a larger enhancement in the LDA. The trends seen in the valence-electron enhancement factors can be explained in terms of the changes in the average electron density in the interstitial region, which depends on the volume per atom in the lattice.

It is interesting to compare the positron annihilation characteristics for the bulk II–VI compound semiconductors with those for the group II metals Zn, Cd and Hg. In order to simplify calculations and comparisons, the hexagonal Zn, Cd and the rhombohedral Hg have been built as FCC lattices with the true Wigner–Seitz volumes. The lattice constants of these theoretical FCC metals are given in table 1. The results from the atomic superposition calculations for the annihilation rates and the enhancement factors are given in tables 3 and 4. The annihilation rates are discussed below in the context of the comparison with experimental results. A comparison of the enhancement factors for the metals with those for the group II atoms in II–VI compound semiconductors shows interesting trends. First, the core enhancement factors in both cases are very similar in magnitude and follow the same trends. Secondly, figure 2(*b*) shows that, in spite of the very different lattice structures, the enhancement factors for the d electrons in the different metals follow the same trends as a function of the volume per atom as those for the corresponding group II atoms in the compound semiconductors. Moreover, the calculated core enhancement factors for Zn and Cd agree with the values obtained by Jensen [34] using the Wigner–Seitz sphere approximation and with those calculated using the true HCP geometry [36]. However, the value obtained by Sob [37] in a semiempirical theory for Zn is remarkably smaller than the LDA values.

Equation (4) accounts for incomplete screening by decreasing the total annihilation rate by the constant factor of $2.01/\epsilon_\infty$. For the II–VI compound semiconductors this means an increase in the positron lifetimes by about 10–20 ps. The variation of the high-frequency dielectric constant between the different materials also causes some trends. The most remarkable is the decrease of the positron lifetime between the Cd and Hg series (figure 1). About half of this decrease is due to the increase of the dielectric constant. The slight decrease of the slopes of positron lifetimes in figure 1 when going from the Zn series to the Cd series and further to the Hg series is also caused by the behaviour of the dielectric constant. The screening correction lowers the local enhancement by $r_s^3/(6\epsilon_\infty)$. Because this is inversely proportional to the electron density, it mainly affects the valence enhancement factor and annihilation rate. The correction does not affect the above-discussed trends due to the variation of the volume per atom in the lattice or due to the variation of the extent of the d-electron density.

3.2. $Cd_{1-x}Hg_xTe$ ternary compound

The ternary compound semiconductor $Cd_{1-x}Hg_xTe$ is one of the most important infrared detector materials. The positron technique has also been used to study its properties [8–10]. In order to analyse the results obtained by the positron annihilation method, it is important to know the positron bulk lifetime of this compound as a function of the Hg concentration x. Our aim is to give a practical interpolation formula for the positron bulk lifetime. There is, however, one difficulty. The dielectric constant of the compound depends strongly on x, but the dependence is not known accurately. Therefore we have made calculations for the positron lifetime by treating both the dielectric constant and the Hg concentration as parameters. Because the two extremes of the alloy, CdTe and HgTe, have nearly the same lattice constant, we have assumed in the calculations that the lattice parameter of the ternary compound depends linearly on x. The calculations are performed for ordered lattices.
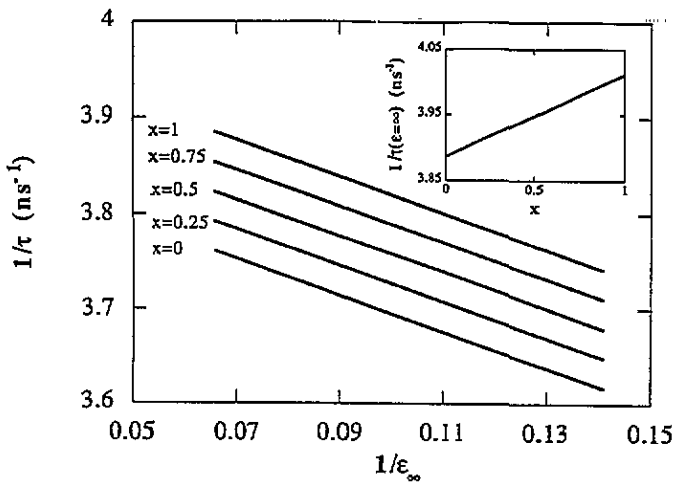

Figure 3. Positron annihilation rate $(1/\tau)$ for the ternary compound semiconductor $Cd_{1-x}Hg_xTe$ as a function of the inverse of the high-frequency dielectric constant and for different Hg contents. The inset shows the dependence of the annihilation rate on the Hg content for the metallic limit $(\epsilon_\infty = \infty)$.

Figure 3 shows the calculated total annihilation rates as a function of $1/\epsilon_\infty$ for different contents x. The linear relations obtained are related to the linear dependence, $\Gamma(n(r)) \propto -2.01/\epsilon_\infty$, in equation (4). However, because the correlation potential also depends on ϵ_∞ [23], the actual calculated slope is slightly smaller, very nearly equal to -1.91. For a given value of $1/\epsilon_\infty$ the total annihilation rate depends linearly on x. For example, in the inset of figure 3 this linear dependence is shown for $1/\epsilon_\infty = 0$ (corresponding to metallic screening). By making linear fits with respect to x and $1/\epsilon_\infty$, we obtain for the total annihilation rate (in ns^{-1}) the interpolation formula

$$1/\tau = 0.12x - 1.91/\epsilon_\infty + 3.89. \tag{8}$$

This equation shows that the annihilation rate increases linearly with the Hg content and decreases linearly with the inverse of the dielectric constant of the compound.

3.3. Comparison with experiments

Experimental data for positrons in II–VI compound semiconductors are quite scarce. We have found experimental data for only five compounds, ZnS, ZnSe, ZnTe, CdTe and HgTe (see table 1). CdTe has received the largest attention, and the proposed bulk lifetimes range

from 278 to 291 ps [7, 8, 12–14]. In the case of the other four compound semiconductors, the proposed bulk lifetimes are: $\tau_b = 230 \pm 3$ ps for ZnS [15], $\tau_b = 240 \pm 5$ ps for ZnSe [15], $\tau_b = 266 \pm 3$ ps for ZnTe [16] and $\tau_b = 274 \pm 1$ ps for HgTe [8]. The present calculated values are consistently slightly shorter than the experimental ones. The largest relative difference is 6% in the case of HgTe and the smallest one is 3% for CdTe (here we compare with the average of the experimental values, i.e. with $\tau_{exp}^* = 284$ ps for CdTe). The calculated positron lifetimes for Zn, Cd and Hg metals are 138, 157 and 153 ps, respectively. These values are also systematically shorter than the experimental ones of 148, 175 and 182 ps, respectively. Moreover, the LDA results [33, 34] for the noble metals and for the late transition metals usually are shorter than the experimental ones (experimental results have been collected for example in [38]).

The too short LDA lifetimes for solids having relatively delocalized d-electron bands near the Fermi energy suggest that the LDA overestimates their enhancement factors. The similarity of the results obtained in atomic superposition and LMTO-ASA calculations means that the effect does not depend strongly on the self-consistency of the electron structure. Moreover, the trends in figure 2(*b*) for the enhancement factor of the group II atom d electrons indicate that the enhancement is related to the extent of the d-electron density. Therefore the enhancement as well as its overestimation in the LDA are largely properties of the atom in question and depend only weakly on the host where the atom sits. In order to test the validity of these ideas, we have determined the d-electron enhancement factors for Zn, Cd and Hg metals so that the calculated positron lifetimes agree with the experimental ones. By scaling the enhancement factors for the group II d electrons in the compound semiconductors by the same factors as for the corresponding metals, we obtain new semiempirical enhancement factors and positron lifetimes. The results are collected in table 5. The resulting d-electron enhancement factors are typically about 10–20% larger than the core enhancement factors, whereas within LDA the corresponding number is about 50–60%. The new semiempirical positron lifetimes for ZnS, ZnSe, ZnTe, CdTe and HgTe agree rather well with the experimental ones. It is especially gratifying to note that the semiempirical procedure causes the largest lifetime increase in the case of HgTe for which the LDA underestimation is the worst. The good agreement between the semiempirical and experimental lifetimes for II–VI compound semiconductors strongly supports the idea that the LDA fails in treating the annihilation with the delocalized d electrons whereas it describes reasonably well the annihilation rates with both inner core and outer valence electrons.

There are a few experimental values for the positron bulk lifetimes in the ternary compounds $Cd_{1-x}Hg_xTe$. For $Cd_{0.2}Hg_{0.8}Te$ lifetimes in the rather wide range of 265–286 ps have been proposed [8–10]. For the compound $Cd_{0.27}Hg_{0.73}Te$ the relatively long lifetime of 284 ps has been determined [10]. Because of the large scatter the comparison of the experimental values with the theoretical ones is difficult. With interpolated values for the high-frequency dielectric constant (equation (8)), shorter values than the proposed experimental ones are obtained. This is because the calculated values for CdTe and HgTe are already shorter than the experimental ones. If the experimental (τ_{exp}^*) or semiempirical lifetimes for CdTe and HgTe are used in fitting equation (8), the direct dependence on x practically vanishes, because these lifetimes are much closer to each other than the LDA values for CdTe and HgTe. This means that all the dependence on x in the ternary compounds would come through the variation of the high-frequency dielectric constant and the direct dependence on x would only be an artefact due to LDA. A systematic experimental study of the dependence of the positron lifetime on the composition and on the high-frequency dielectric constant could clarify the situation. However, the theoretical trend that the positron lifetime decreases when Cd is substituted by Hg seems clear.

Table 5. Result obtained for the perfect II–VI compound semiconductors and group II metal lattices by using for the d electrons of the group II atoms scaled enhancement factors $(\gamma_d^{II})'$. The scaling is performed so that the experimental positron lifetimes for Zn, Cd and Hg metals are reproduced. τ' are the corresponding positron lifetimes.

Host	$(\gamma_d^{II})'$	τ' (ps)
ZnS	2.44	225
ZnSe	2.49	240
ZnTe	2.57	260
CdS	2.50	254
CdSe	2.55	265
CdTe	2.63	286
HgS	2.47	249
HgSe	2.55	258
HgTe	2.61	274
Zn	2.38	148
Cd	2.43	175
Hg	2.30	182

The LDA for the positron annihilation rate systematically overestimates the annihilation rate with the outer d electrons in very different types of materials. A systematic improvement would require non-local terms in the theory. The situation is analogous to the use of the LDA for electron exchange and correlation in electronic structure calculations [39], in which a typical LDA error is the overestimation of the binding energies. Similar techniques to those used for electronic structure calculations could in principle be used also to describe the screening cloud around the positron in a non-uniform electron system. The so-called weighted density approximation (WDA) [40] has already been applied in the case of a positron outside a jellium surface [41] or inside a jellium vacancy [42]. An appealing approach would be corrections employing the gradients of the electron density [43]. These methods (see for example [44]) have recently attracted a lot of interest in electronic structure calculations. The gradient corrections to the screening cloud around the positron are expected to affect remarkably the annihilation with the outer d electrons because their density changes rapidly rather far away from the nuclei, and therefore this rapid change is efficiently seen by the positron.

4. Positron trapping at vacancies and divacancies

In this section we present results for vacancies and nearest-neighbour divacancies in II–VI compound semiconductors. The lattice relaxation around the defect is not taken into account. Moreover, the atomic superposition used in the calculations does not allow the description of differences in the electronic structures between the different charge states of the defect. However, it has been shown that charge state affects the positron lifetime mainly through the changes in the atomic relaxations [3, 45]. Therefore, if the relaxed positions of the atoms around the defect are known, the atomic superposition method can be used to estimate the positron lifetimes. A crucial point in this context is that the atomic relaxation due to the trapped positron itself should in principle be taken into account [28]. This is a major theoretical and computational task, which is difficult to access with the present-day

theoretical models and computer resources, especially if one is interested in studying the general trends. Therefore, in the present work, we will omit the lattice relaxation and the positron-induced changes in the electronic structure beyond the short-range enhancement.

Table 6. Positron annihilation characteristics for monovacancies and nearest-neighbour divacancies in II–VI compound semiconductors. λ_c, λ_v and λ_d are the annihilation rates due to the core, valence and d electrons, respectively. E_b is the positron binding energy at the defect and τ is the positron bulk lifetime. A_d/A_b is the ratio of relative numbers of core and d-electron annihilations (see equation (9)) between the defect and bulk states.

Host	Defect	λ_c (ns^{-1})	λ_v (ns^{-1})	λ_d (ns^{-1})	E_b (eV)	τ (ps)	A_d/A_b
ZnS	V_{Zn}	0.141	3.588	0.556	0.11	233	0.850
ZnSe	V_{Zn}	0.125	3.393	0.569	0.08	245	0.895
ZnTe	V_{Zn}	0.107	3.199	0.521	0.05	261	0.934
CdS	V_{Cd}	0.120	3.034	0.614	0.12	265	0.802
CdSe	V_{Cd}	0.110	2.947	0.617	0.09	272	0.845
CdTe	V_{Cd}	0.095	2.821	0.560	0.06	288	0.895
HgS	V_{Hg}	0.133	2.977	0.922	0.10	248	0.849
HgSe	V_{Hg}	0.120	2.940	0.900	0.07	253	0.879
HgTe	V_{Hg}	0.105	2.846	0.799	0.05	267	0.911
ZnS	V_S	0.166	3.475	0.706	0.08	230	1.048
CdS	V_S	0.159	3.013	0.849	0.05	249	1.032
HgS	V_S	0.166	2.888	1.193	0.05	235	1.038
ZnSe	V_{Se}	0.135	3.178	0.653	0.10	252	1.048
CdSe	V_{Se}	0.134	2.854	0.782	0.06	265	1.037
HgSe	V_{Se}	0.140	2.781	1.101	0.07	249	1.054
ZnTe	V_{Te}	0.096	2.810	0.532	0.18	291	1.040
CdTe	V_{Te}	0.099	2.589	0.637	0.11	301	1.052
HgTe	V_{Te}	0.106	2.525	0.932	0.12	281	1.101
ZnS	Divac	0.089	2.916	0.424	0.47	292	0.782
ZnSe	Divac	0.075	2.749	0.403	0.45	310	0.781
ZnTe	Divac	0.058	2.588	0.341	0.48	335	0.760
CdS	Divac	0.083	2.571	0.498	0.40	317	0.759
CdSe	Divac	0.071	2.487	0.467	0.40	331	0.759
CdTe	Divac	0.055	2.374	0.390	0.41	355	0.750
HgS	Divac	0.091	2.508	0.764	0.37	297	0.826
HgSe	Divac	0.077	2.478	0.712	0.37	306	0.825
HgTe	Divac	0.060	2.375	0.603	0.41	329	0.825

4.1. Positron lifetimes

The annihilation rates, lifetimes and binding energies for positrons trapped by vacancies and divacancies are collected in table 6. These results correspond to the LDA for positron annihilation with the dielectric correction (equation (4)). The use of the semiempirical correction for the d-electron enhancement scales the lifetimes to longer values but does not

affect the overall trends. Figures 4–6 show the wavefunction of a positron trapped by the two kinds of vacancies and the nearest-neighbour divacancy in CdTe. The localization in the vacancies is much weaker than in typical metal vacancies (see figure 4). In fact, the increase of the positron lifetime from the bulk state to the vacancy state is quite small in all materials. The ratio between the positron lifetimes at monovacancies and in bulk is 1.02–1.14 (for divacancies about 1.28–1.33). For metals the ratio is typically around 1.5–1.6, reflecting a more localized positron wavefunction. Therefore, an open volume of more than a divacancy is needed to maintain localization similar to that at metal vacancies. Figure 7 shows that the positron lifetimes corresponding to (neutral) vacancies and divacancies increase linearly as a function of the volume per atom in the lattice. However, the increase depends on the type of vacancy defect. It is steepest for the group VI atom monovacancies (V_{VI}) and lowest for the group II atom monovacancies (V_{II}). The lifetimes for the divacancies show similar trends to the bulk lifetimes in figure 1. In the case of the V_{II} monovacancies as well as in the case of the V_{VI} monovacancies, three groups corresponding to Zn, Cd and Hg series can be separated. Within each of the series the slope corresponding to the V_{VI} monovacancies is larger than that for the V_{II} monovacancies because in the former case the size of the missing atom increases. Note the similarity, apart from a nearly constant shift, between the Cd and Hg series in figure 7. This similarity is a result of the nearly equal sizes of the Cd and Hg atoms (cf the FCC lattice constants for Cd and Hg metals in table 1).
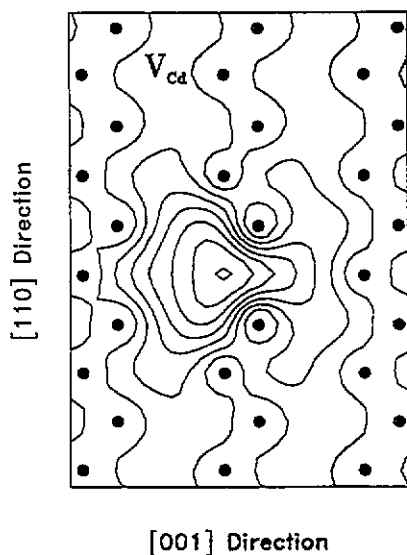

Figure 4. Positron wavefunction in the Cd vacancy in CdTe. The ion positions are denoted by full circles. The contour spacing is 1/8th of the maximum value.
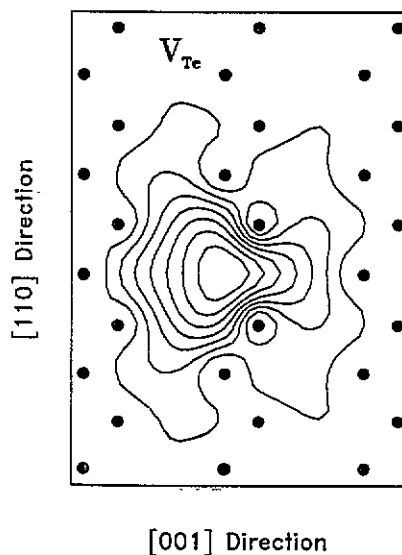
Figure 5. Positron wavefunction in the Te vacancy in CdTe. The ion positions are denoted by full circles. The contour spacing is 1/8th of the maximum value.

The positron binding energies at monovacancies are very low, about 0.05–0.15 eV (table 6). The low binding energy results in a relatively delocalized character of the positron wavefunction and a small lifetime increase from the bulk value. For divacancies, the binding energies are larger, about 0.4 eV, indicating a substantially better localization than in the case of monovacancies. However, one should bear in mind that the positron binding energy to a defect is quite sensitive to the self-consistency of the electronic structure. Moreover, if
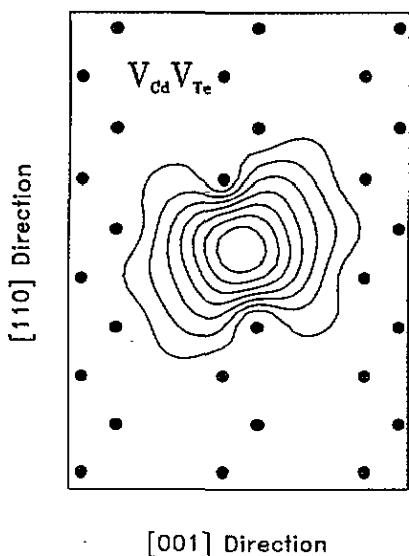
Figure 6. Positron wavefunction in the nearest-neighbour divacancy in CdTe. The ion positions are denoted by full circles. The contour spacing is 1/8th of the maximum value.
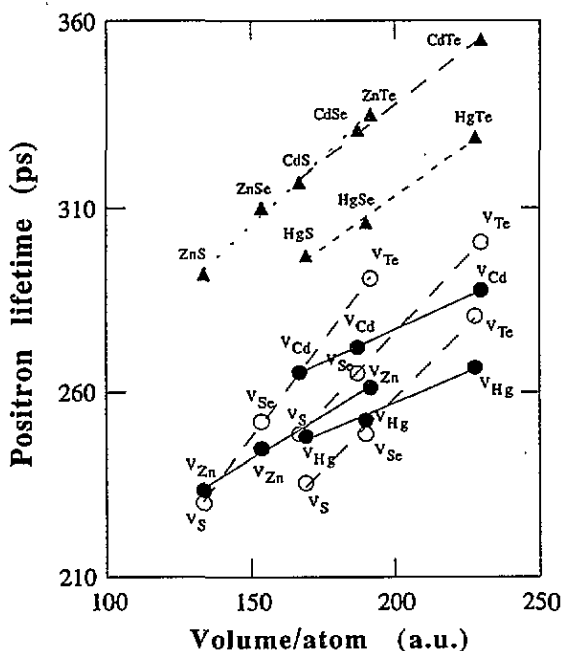

Figure 7. Positron lifetimes for the group II atom vacancies (●), the group VI atom vacancies (○) and the nearest-neighbour divacancies (▲) as a function of the volume per atom in the lattice. The full lines are linear fits to the group II atom vacancies and the broken lines to the group VI atom vacancies and divacancies for the Zn, Cd and Hg series of II–VI compound semiconductors.

the effects due to the localized positron were included self-consistently, the positron binding energy would increase due to the increase of the average electron density [26] and the lattice relaxation [28] at the defect.

Experimental positron lifetime data for vacancies exist only for ZnS, ZnSe, CdTe and HgTe. The large variety of different vacancy-type defects makes the assignment of measured lifetimes to specific defects very difficult. Moreover, depending on the position of the Fermi level, the defects may be in different charge states. This fact may lead, owing to the charge-state dependence of the lattice relaxation, to different positron lifetime values for different

charge states. However, depending on the sample conditions, some of the defects can be excluded from the analysis. A typical case is a positively charged defect, which does not trap positrons [46]. Specifically, in the case of II–VI compound semiconductors, the group VI vacancies are expected to be positive unless the Fermi level is in the upper half of the band gap [17].

The theoretical positron lifetimes for vacancies given in table 6 are typically much shorter than the corresponding experimental lifetimes suggested. The discrepancy is partly due to the LDA, which gives too short positron lifetimes already for the bulk state. If one uses for the d-electron enhancement the semiempirical correction, which gives positron bulk lifetimes in good agreement with experiments, the positron lifetimes for vacancy defects become longer. However, we have found it convenient, instead of comparing directly the experimental and theoretical positron lifetimes, to calculate the ratios between the defect and bulk lifetimes and compare them with experiment. The calculated ratios are much less sensitive to the approximations used for the enhancement, and some systematic errors in the measured lifetimes are expected to cancel in the ratios.

For ZnS two long-lifetime components of 266 and 286 ps have been measured [15]. Assuming that these lifetimes are too low for divacancies, they have been assigned to the doubly and singly negative Zn monovacancy, respectively [15]. Also in the case of ZnSe the two measured lifetime components of 270 and 300 ps have been correlated with the doubly and singly negative Zn monovacancies, respectively [15]. Thus, according to these measurements the positron lifetimes for the doubly negative Zn monovacancies are approximately by a factor 1.13–1.16 longer than the positron bulk lifetimes (see table 1). The corresponding factor for the singly negative Zn monovacancies is about 1.24–1.25. The theoretical positron results in table 6 indicate that the positron lifetime for the Zn vacancies should be only about 1.05–1.06 and the lifetime for the divacancies about 1.32–1.33 times the bulk lifetime. Combining the experimental and theoretical results, the open volume seen by the positron at real defects should be between the open volumes for the ideal (i.e. no lattice relaxation) mono- and divacancies. According to this result, we expect also that a fully self-consistent calculation of the electronic and ionic structure of the defect and the positron state can result in a better agreement with experiment.

Electron-irradiated CdTe shows a long-positron-lifetime component of 325 ps [8], which has also been found in as-grown materials (320 ps [14], 330 ps [8]). In as-grown, p-type or semi-insulating materials, another long-lifetime component of 385 ps has also been found [8]. Even though there is no agreement between different authors, these lifetime components have been assigned to defects related to Cd monovacancies [8, 12–14]. In as-grown HgTe a long component of 316 ps has also been found [8]. The positron lifetimes around 320 ps are by a factor of 1.13–1.16 longer than the corresponding positron bulk lifetimes. The lifetime component of 385 ps is by a factor 1.36 longer than the measured bulk lifetime. The corresponding theoretical factors from table 6 are 1.04 for Cd or Hg vacancies, 1.09 for Te vacancies, and 1.28 for divacancies in both CdTe and HgTe. Comparing the theoretical and experimental lifetime ratios, we believe that the measured positron lifetimes around 320 ps correspond to vacancies but the lifetime component of 385 ps should be connected with a divacancy. In both cases the fully self-consistent electronic structure and lattice relaxation should increase the positron lifetime. In fact, the existence of divacancies in CdTe and the sensitivity of positrons to them have recently been demonstrated by Doppler lineshape measurements for CdTe films using a slow-positron beam [18].

4.2. Core annihilation parameter

Doppler broadening of the annihilation line has been successfully used in the identification

of defects in semiconductors [18–20]. The Doppler lineshape measurement is especially valuable in the case of thin films, which cannot be measured by the conventional lifetime techniques because of the large penetration of the energetic positrons. The lineshape is usually analysed using the so-called lineshape parameters S and W. The S parameter is the relative number of annihilation events in a certain energy region near the centre of the peak. The W parameter is the relative number of annihilation events in a certain energy region in the tail part of the annihilation line. The S parameter corresponds mainly to annihilation with low-momentum valence electrons, whereas only the high-momentum core (including the filled d bands) electrons contribute to the W parameter. The trapping by vacancies is seen as an increase of the S parameter and a decrease of the W parameter. Especially, analysis of the changes in the W parameter relative to its bulk value has turned out to be very useful in the identification of defects [18–20]. Moreover, the existence of different types of defects in different samples can be observed when the S parameter is plotted as a function of the W parameter [18]. Namely, if it is assumed that each of several samples contains mainly one type of defect, but its concentration and consequently the ratio of positrons annihilating from it vary from sample to sample, the data points corresponding to the same defect fall on the same straight line in the S versus W plot.

The calculated positron annihilation rates can be compared with the measurements of the W parameters to support the defect identification [18]. First the relative number of annihilations with core and d electrons is calculated as

$$A_i = \frac{\lambda_c + \lambda_d}{\lambda_c + \lambda_d + \lambda_v} \tag{9}$$

for the bulk ($i = $ b) and defect ($i = $ d) states. Instead of comparing the absolute values, one calculates the ratio A_d/A_b between the defect state in question and the bulk state and similarly the ratio between the W parameters for the sample with defects and for the reference sample without defects. These theoretical and experimental ratios can be compared with each other.

The ratios A_d/A_b between the defect and bulk states are given in table 6. These values have been calculated using the annihilation rates obtained in the LDA, but if the semiempirical correction for the d enhancement is used the values do not change remarkably. In the case of V_{II} vacancies the relative contribution of the core and d electrons to the total annihilation rate is less than in the perfect bulk lattice and the A_d/A_b ratios are in the range of 0.80–0.93. For the divacancies the relative importance of the core and d-electron annihilation decreases further, and the A_d/A_b ratios are about 0.75–0.83. In the case of the V_{VI} vacancies it is interesting to note that the A_d/A_b ratios are larger than unity, about 1.03–1.10. For the Hg series even the absolute value of the sum of the core and d-electron annihilation rates is larger for the V_{VI} vacancy than for the bulk. The large A_d/A_b ratios for the V_{VI} vacancies reflect the fact that the trapped positron overlaps strongly with the core electrons of the four atoms neighbouring the vacancy. In the case of the V_{VI} vacancies, these are group II atoms with relatively extended d-electron densities. Thus we may conclude that, if positrons are trapped by the V_{VI} vacancies, the measured W parameter should increase. The trapping of a positron by the V_{VI} vacancies is, however, impossible if these vacancies are in positive charge states.

The above discussion shows that the measurement of the W parameter can be an effective tool in identifying defects in semiconductors. For example, the W parameter measurements have been performed for thin CdTe films by Liszkay *et al* [18]. They distinguished two different defects with the defect to bulk ratios of the W parameters as 0.85 and 0.72. According to table 6 these values can be connected with the Cd vacancy and the divacancy

for which the theoretical A_d/A_b ratios are 0.90 and 0.75, respectively. This agrees with the identification by Liszkay *et al.* The slightly larger theoretical values may reflect the too delocalized characters of the positron states at the defects.

5. Conclusions

We have estimated the positron bulk lifetimes and the lifetimes for vacancy-type defects in II–VI compound semiconductors using for the positron annihilation rate the LDA and the screening correction, which depends on the high-frequency dielectric constant. By studying systematically the trends between the different compounds, our aim has been to support the experimental work for defect characterization and, on the other hand, by comparison with experimental positron lifetimes to test the validity of the theoretical methods.

The calculated bulk lifetimes are systematically shorter than their experimental counterparts, which have been proposed for five different semiconductors. The difference between the experimental and theoretical values is traced back to the overestimation of the enhancement factor for the electrons on the energy bands originating from the highest d orbitals of the group II atoms in the compound. This overestimation in the d-electron enhancement factor in the LDA is about 30%. This value is found to be quite insensitive to the environment of the group II atom. The characteristic feature of the density of the highest d electrons is its rapid variation in the interstitial region important for the positron annihilation. Therefore we conclude that corrections beyond the LDA are needed in describing positron annihilation in solids with d bands relatively high in energy.

The positron states at monovacancies, calculated without allowing the atoms to relax from their ideal lattice positions, are quite delocalized and the lifetimes for monovacancies are only slightly longer than the bulk lifetimes. More detailed calculations would require that the lattice relaxation and the changes in it induced by the trapped positron are fully taken into account. However, already the comparison of the present calculated positron lifetimes with the measured ones gives an idea about the open volume seen by the positron at the defect and an idea how it is expected to change between the different vacancy defects and compounds. The comparison of the calculated relative (with respect to the bulk value) core annihilation rate contributions with the measured relative W parameters also gives valuable information for defect identification. The present results show that changes in the positron lifetime and in the core annihilation contributions are quite insensitive to the details of the theory if the changes are calculated as ratios between the parameters for the defects and those for the perfect bulk lattice.

Finally, we underline again that experimental positron results exist thus far only for a few II–VI compound semiconductors. New experimental results would help the interpretation of the existing experimental findings and the development of the theory for positron states and annihilation.

References

[1] Mäkinen J, Corbel C, Hautojärvi P, Moser P and Pierre F 1989 *Phys. Rev.* B **39** 10 162
[2] Dannefaer S, Mascher P and Kerr D 1986 *Phys. Rev. Lett.* **56** 2195
[3] Puska M J, Jepsen O, Gunnarsson O and Nieminen R M 1986 *Phys. Rev.* B **34** 2695
[4] Puska M J 1987 *Phys. Status Solidi* a **102** 11
[5] Corbel C, Pierre F, Saarinen K, Hautojärvi P and Moser P 1992 *Phys. Rev.* B **45** 3386
[6] Hautojärvi P, Moser P, Stucky M, Corbel C and Plazaola F 1986 *Appl. Phys. Lett.* **48** 809

Dannefaer S 1982 J. Phys. C: Solid State Phys. 1 599

[8] Geffroy B, Corbel C, Stuck M, Triboulet R, Autojärvi P, Plazola F, Saarinen K, Rajainmäki H, Hautojärvi J, Moser P, Sengupta A and Pautrat J L 1986 Mater. Sci. Forum 10–12 1241

[9] Krause R, Polity A, Klimakow A and Scherz U 1993 Positron Annihilation (Singapore: World Scientific) p 684

[10] He Y J, Li X F, Li L H, Yu W Z and Xia Y 1993 J. Phys.: Condens. Matter 1 SA97

[11] Gély C, Corbel C and Triboulet R 1990 J. Phys.: Condens. Matter 2 413

[12] Geffroy B 1983 Rapport CEA R 19

[13] Gély C, Corbel C and Triboulet R 1989 C.R. Acad. Sci. Paris 309 II, 79

[14] Gély Sykes C, Corbel C and Triboulet J 1993 Solid State Commun. 31 79

[15] Pareja R, de la Cruz M and Moser P 1992 J. Phys.: Condens. Matter 4 113

[16] de la Cruz M, Pareja R and Moser P 1992 Mater. Sci. Forum 10 110 151

[17] Tapohi P and Ray S 1983 Prog. Cryst. Growth Charac. 7 103 v 62

[18] Liszkay L, Corbel C, Baroux L, Hautojärvi P, Bayhan M, Brinkman A W and Tatarenko S 1994 Appl. Phys. Lett. 64 1380

[19] Mäkinen J, Laine T, Saarinen K, Hautojärvi P, Corbel C, Airaksinen V M and Gibart P 1993 Phys. Rev. Lett. 71 3154

[20] Saarinen K, Kuisma S, Hautojärvi P, Corbel C and LeBerre C 1994 Phys. Rev. 49 8005

[21] Landolt-Bornstein 1985 Physics of I-VI and I-VII Compounds vol 17 (subvol b) (Berlin: Springer)

[22] Laks D B, Van de Walle C G, Neumark G F, Blöchl P E and Pantelides S 1992 Phys. Rev. B 45 11965

[23] Puska M J, Mäkinen S, Manninen M and Nieminen R M 1989 Phys. Rev. B 29 7666

[24] Puska M J and Nieminen R M 1994 J. Phys. F: Met. Phys. 13 333

[25] Andersen O L, Jepsen C and Glötzel M 1985 Electronic Band Structure and its Applications ed M Yussouf (Heidelberg: Springer) p 1

[26] Boronski E and Nieminen R M 1986 Phys. Rev. B 34 3820

[27] Laasonen K, Nieminen R M and Puska M J 1992 Phys. Rev. B 44 1122

[28] Laasonen K, Alatalo M, Puska M J and Nieminen R M 1991 J. Phys.: Condens. Matter 3 7217

[29] Arponen J and Pajanne E 1979 J. Phys. F: Met. Phys. 9 2359

[30] Gilgien D H and Allen B 1990 Phys. Rev. Lett. 45 165

[31] Krew J and Zunger A 1983 Phys. Rev. B 27 1048

[32] Kimball J E and Shortley G 1934 Phys. Rev. 45 815

[33] Puska M J 1991 J. Phys.: Condens. Matter 3 1455

[34] Jensen K O 1989 J. Phys.: Condens. Matter 1 10595

[35] Arponen J and Pajanne E 1985 Positron Annihilation ed P C Jain, R M Singru and K P Gopinathan (Singapore: World Scientific) p 21

[36] Daniuk S, Sob M and Rubaszek A 1991 Phys. Rev. B 43 2580

[37] Sob M 1985 Solid State Commun. 53 255

[38] Seeger A, Banhart F and Bauer W 1989 Positron Annihilation ed L Dorikens-Vanpraet, M Dorikens and D Segers (Singapore: World Scientific) p 275

[39] Jones R O and Gunnarsson O 1989 Rev. Mod. Phys. 61 689

[40] Gunnarsson O, Jonson M and Lundqvist B I 1979 Phys. Rev. B 20 3136

[41] Jensen K O and Walker A B 1988 J. Phys. F: Met. Phys. 18 L277

[42] Gilgien D, Jensen K O and Walker A B 1991 J. Phys.: Condens. Matter 3 2049

[43] Nieminen R M 1993 Private communication

[44] Perdew J P, Chevary J A, Vosko S H, Jackson K A, Pederson M R, Singh D J and Fiolhais C 1992 Phys. Rev. B 46 6671

[45] Mäkinen S and Puska M J 1989 Phys. Rev. B 40 12523

[46] Puska M J, Corbel C and Nieminen R M 1990 Phys. Rev. B 41 9980

[47] Hidalgo C, de Diego N and Moser P 1985 Appl. Phys. A 40 175

[48] Puff W and Panzer P 1984 J. Phys. F: Met. Phys. 14 L231

[49] West R N, Cooper V H, DeBlaere G and Hogg B G 1973 Phys. Lett. 45A 141